

LA-UR-00-3331

Approved for public release;
distribution is unlimited.

Title: INTEGRATING INTERPOLATION FUNCTIONS
ACROSS TRIANGULAR AND QUADRILATERAL
CELL BOUNDARIES

Author(s) J. Renae Wiseman, U. S. Air Force Academy
Jerry S. Brock, Los Alamos National Laboratory

Submitted: October 2000

Los Alamos
NATIONAL LABORATORY



Photograph by Chris J. Lindberg

Los Alamos National Laboratory, an affirmative action/equal opportunity employer, is operated by the University of California for the U.S. Department of Energy under contract W-7405-ENG-36. By acceptance of this article, the publisher recognizes that the U.S. Government retains a nonexclusive, royalty-free license to publish or reproduce the published form of this contribution, or to allow others to do so, for U.S. Government purposes. The Los Alamos National Laboratory requests that the publisher identify this article as work performed under the auspices of the U.S. Department of Energy. Los Alamos National Laboratory strongly supports academic freedom and a researcher's right to publish; as an institution, however, the Laboratory does not endorse the viewpoint of a publication or guarantee its technical correctness.

Integrating Interpolation Functions Across Triangular and Quadrilateral Cell Boundaries

J. Renae Wiseman, Mathematics Department
U. S. Air Force Academy, Colorado Springs, CO 80841

Jerry S. Brock, Applied Physics Division
Los Alamos National Laboratory, Los Alamos, NM 87545

Abstract

Computational models of particle dynamics often exchange solution data with discretized continuum-fields using interpolation functions. These particle methods require a series expansion of the interpolation function for two purposes: numerical analysis used to establish the models consistency and accuracy, and logical-coordinate evaluation used to locate particles within a grid. This report presents *discrete-expansions* for multi-linear interpolation functions as defined in triangular and quadrilateral cells. Application of the linear and bilinear discrete-expansions for numerical analysis and localization in particle methods is outlined and discussed.

Integrating Interpolation Functions Across Triangular and Quadrilateral Cell Boundaries

Introduction

Particle methods, computational models of particle dynamics, are often solved concurrently with discretized continuum-field equations. Interactive particle methods, including models of liquid sprays [1-4], bubble dynamics [5-9], and material-interface tracking [10,11], strongly couple the governing equations through the bilateral exchange of mass, momentum, and energy. In contrast, reactive particle methods, including models of atmospheric transport [12-19], porous-media diffusion [20-29], and transient mixing [30-32], weakly couple the governing equations; reactive particles simply respond to the entraining continuum field. Another reactive method, used extensively for solution visualization [33-35], free-surface tracking [36-41], and front tracking [42-48], is the tracer-particle method which advects a massless particle with an interpolated velocity [49-57]. Both interactive and reactive particle methods exchange solution data with discrete fields using interpolation functions. The focus of this research was on the role of two common interpolation functions used within existing particle methods.

Particle methods often use interpolation functions directly to evaluate terms in their governing equations. A Taylor's series of the interpolation function, expanded from the particle's cell, is required to perform analytical studies of these numerical methods. The numerical analyses include establishing the models mathematical consistency and numerical accuracy. The particle's equations, including kinematic equations-of-motion, are often numerically integrated using multi-step methods such as Runge-Kutta methods. The interpolated quantities that appear within the particle's discretized equations may be evaluated in a neighboring cell, and the required interpolation expansion would then extend through multiple cells in the grid. Derivatives of interpolation functions, however, are generally not continuous across cell boundaries and, therefore, a Taylor's series is not valid in this situation. An alternative expansion for interpolation functions is required to complete numerical analyses for these particle methods.

Particle methods also often use interpolation functions indirectly to evaluate particle-grid connectivity data: the identity of the grid cell in which the particle resides and the particle's logical-coordinate position vector relative to that cell. Particle localization establishes this data using cell-searching and logical-coordinate evaluation methods [58-63]. Cell-searching methods typically use the particle's logical coordinates to both direct and halt the search. Logical-coordinate evaluation involves transforming a physical-space position vector into a local coordinate system, and, as described below, existing methods are based on interpolation expansions. Particle methods, therefore, require the expansion of interpolation functions for

numerical analysis and localization, and the mathematical expression required for both purposes is identical; the methods developed herein are, therefore, valid for both purposes.

While multi-cell Taylor's series of interpolation functions are not valid for numerical analyses, modified versions of these expansions are used for particle localization. For spatial-transformation, the arguments of the interpolation function include logical-coordinate and cell-vertex coordinate vectors. Existing logical-coordinate evaluation methods, generalized in Reference [58] for various cell geometries, were developed from a truncated, single-variable Taylor's series expansion of the interpolation function [53,58,60,62,63]. The modified Taylor's series avoids the problem of discontinuous interpolation derivatives across cell boundaries by ignoring the function's dependence on the cell-vertex coordinates. Furthermore, the non-linear spatial-transformation problem is linearized by only considering the function's first-order dependence on the logical coordinates. The iterative solution of the resulting system of equations is, however, neither algorithmically robust nor computationally efficient. An alternative expansion for interpolation functions is required for robust and efficient particle localization.

An alternative type of expansion, a *discrete-expansion*, was recently proposed and validated for interpolation functions [64-68]. Discrete-expansions are similar to multi-variable Taylor's series, but the new expansions are valid throughout a discretized domain. Discrete-expansions are valid for numerical analyses since they acknowledge the full functional dependence of interpolation and account for discontinuous derivatives across cell boundaries. Furthermore, the solution of discrete-expansions for logical-coordinate evaluation is both algorithmically robust and computationally efficient. Using a simple finite-difference technique, a single discrete-expansion was developed for trilinear interpolation defined within three-dimensional hexahedral cells [64-66]. More recently, multiple discrete-expansions were developed for linear and bilinear interpolation functions defined within triangular [67] and quadrilateral cells [68]. These two-dimensional discrete-expansions were developed using a generalized and mathematically rigorous total-differential technique. While the total-differential development method is dimensionally independent, the technique produced different forms and, thus, features of the discrete-expansions for linear and non-linear interpolation functions.

The purpose of this report is to first review, then compare and contrast discrete-expansions for linear and bilinear interpolation. This report continues by briefly describing the total-differential method of developing discrete-expansions for these functions. Application of the new interpolation expansions for numerical analysis or localization within particle methods is beyond the scope of this report. The utility of the multi-linear interpolation discrete-expansions for these purposes, however, is outlined and discussed, and a summary concludes this report.

Multi-Linear Interpolation

Two-dimensional computational space is frequently discretized into either triangular or quadrilateral cell geometries. Multi-linear functions are often applied within these cells for both data interpolation and spatial-transformation. Interpolation produces a continuous mapping of discrete field data, often located at cell-vertices, to any position within the cell. The coupling of multiple cell-based interpolation functions across the entire computational domain produces a continuous data field; neighboring multi-linear interpolation functions are continuous along the common boundaries of adjoining cells. Two-dimensional spatial transformation involves mapping from a physical-space, $\bar{X} = (x, y)^T$, to a logical-space, $\bar{\xi} = (\xi, \eta)^T$, coordinate system.

Linear Interpolation

A linear function is generally applied within isoparametric triangular cells; see Figure 1. The linear function is dependent upon both $\bar{\xi}$ and the cell-vertex (cv) coordinate vector for triangles, $\bar{X}^{cv} = ({}^0\bar{X}, {}^1\bar{X}, {}^2\bar{X})^T$, as presented in Equation 1.

$$\begin{aligned} \bar{X}(\bar{\xi}, \bar{X}^{cv}) &= (1 - \xi - \eta) {}^0\bar{X} \\ &+ (\xi) {}^1\bar{X} \\ &+ (\eta) {}^2\bar{X} \end{aligned} \quad (1)$$

Equation 1 is linear with respect to both the logical coordinates, $\bar{\xi}$, and the cell-vertex coordinates, \bar{X}^{cv} . While the physical coordinates of the cell-vertices are arbitrary, the triangle's transformed coordinates are bound by the restrictions $\xi \geq 0$, $\eta \geq 0$, and $\xi + \eta \leq 1$.

Bilinear Interpolation

A bilinear function is generally applied in isoparametric quadrilateral cells; see Figure 2. The bilinear function is dependent upon both $\bar{\xi}$ and the cell-vertex (cv) coordinate vector for quadrilaterals, $\bar{X}^{cv} = ({}^0\bar{X}, {}^1\bar{X}, {}^2\bar{X}, {}^3\bar{X})^T$, as presented in Equation 2.

$$\begin{aligned} \bar{X}(\bar{\xi}, \bar{X}^{cv}) &= (1 - \xi)(1 - \eta) {}^0\bar{X} \\ &+ (\xi)(1 - \eta) {}^1\bar{X} \\ &+ (\xi)(\eta) {}^2\bar{X} \\ &+ (1 - \xi)(\eta) {}^3\bar{X} \end{aligned} \quad (2)$$

Equation 2 is linear with respect to the cell-vertex coordinates, \bar{X}^{cv} , but non-linear with respect to the logical coordinates, $\bar{\xi}$. While the physical coordinates of the cell-vertices are arbitrary, the quadrilateral's transformed coordinates are bound by $0 \leq \xi \leq 1$ and $0 \leq \eta \leq 1$.

Total Differential

Using an interpolation function, $\bar{X}(\bar{\xi}, \bar{X}^{cv})$, the objective is to establish a relationship between the finite change of the physical coordinates, $\Delta\bar{X}$, the logical coordinates, $\Delta\bar{\xi}$, and the cell-vertex coordinates, $\Delta\bar{X}^{cv}$. The function's total-differential provides a relationship between infinitesimal changes of these coordinates, $d\bar{X} = f(d\bar{\xi}, d\bar{X}^{cv})$, as presented in Equation 3.

$$d\bar{X} = \frac{\partial\bar{X}(\bar{\xi}, \bar{X}^{cv})}{\partial\bar{\xi}} d\bar{\xi} + \frac{\partial\bar{X}(\bar{\xi}, \bar{X}^{cv})}{\partial\bar{X}^{cv}} d\bar{X}^{cv} \quad (3)$$

The interpolation function's total-differential includes two derivatives or transformation matrices that are scaled by differential coordinate vectors. The first derivative represents a coordinate-transformation or Jacobian matrix: $\partial\bar{X}/\partial\bar{\xi}$. The size of the square Jacobian matrix is equal to the number of spatial dimensions. The second derivative represents a geometry-transformation matrix: $\partial\bar{X}/\partial\bar{X}^{cv}$. The number of rows and columns in this non-square matrix are equal to the dimension size and the number of elements in the cell-vertex coordinate vector, \bar{X}^{cv} . The size of \bar{X}^{cv} is the problem dimension size multiplied by the number of cell vertices.

The coordinate-transformation matrix for bilinear interpolation is a linear function of both $\bar{\xi}$ and \bar{X}^{cv} . In contrast, the Jacobian matrix for linear interpolation, while linear with respect to \bar{X}^{cv} , is not a function of $\bar{\xi}$. The general, multi-variable description of the Jacobian matrix will be retained for the following development: $\partial\bar{X}(\bar{\xi}, \bar{X}^{cv})/\partial\bar{\xi}$. The geometry-transformation matrix for bilinear interpolation, while not a function of \bar{X}^{cv} , is non-linear with respect to $\bar{\xi}$. In contrast, for linear interpolation, this transformation matrix is linear with respect to $\bar{\xi}$: $\partial\bar{X}(\bar{\xi})/\partial\bar{X}^{cv}$. The interpolation function's simplified total-differential is presented in Equation 4.

$$d\bar{X} = \frac{\partial\bar{X}}{\partial\bar{\xi}}(\bar{\xi}, \bar{X}^{cv}) d\bar{\xi} + \frac{\partial\bar{X}}{\partial\bar{X}^{cv}}(\bar{\xi}) d\bar{X}^{cv} \quad (4)$$

Integration Method

The objective is to integrate the interpolation function's simplified total-differential to obtain a discrete-expansion for interpolation: $\Delta\bar{X} = f(\Delta\bar{\xi}, \Delta\bar{X}^{cv})$. The limits of integration are two particles located in separate, non-contiguous cells: State 1, $\bar{X}_1 = \bar{X}(\bar{\xi}_1, \bar{X}_1^{cv})$, and State 2, $\bar{X}_2 = \bar{X}(\bar{\xi}_2, \bar{X}_2^{cv})$. See Figure 3. Integration of the interpolation function's total-differential between these two particle end-states is represented in Equation 5.

$$\int_1^2 d\bar{X} = \int_1^2 \frac{\partial\bar{X}}{\partial\bar{\xi}}(\bar{\xi}, \bar{X}^{cv}) d\bar{\xi} + \int_1^2 \frac{\partial\bar{X}}{\partial\bar{X}^{cv}}(\bar{\xi}) d\bar{X}^{cv} \quad (5)$$

The linearity of the interpolation function's derivatives affects the complexity of the solution of Equation 5. More importantly, both $\partial\bar{X}/\partial\bar{\xi}$ and $\partial\bar{X}/\partial\bar{X}^{cv}$ must be continuous for the total-differential to be valid within a specified region. Within a single cell, solution of Equation 5 is straightforward; the interpolation derivatives are guaranteed to be continuous in this region. In contrast, if the limits of integration cross a cell boundary, where interpolation functions are continuous but their derivatives are generally discontinuous, the total-differential is not valid. Discrete-expansions can be obtained from Equation 5 if the integration pathline is partitioned into cell-based line-segments, but this technique is prohibitively complex and expensive.

Parameterization

Alternatively, the coordinate-space between the limits of integration can be parameterized. Parameterization removes the concept of multiple coordinate systems and, thus, discontinuous interpolation derivatives, by creating a single coordinate-space between any two particles. The integration pathline end-states can then be defined within any two computational sub-domains, including any two non-contiguous grid cells. While the form of the parameterization function is arbitrary, it must be differentiable; it is embedded in the parameterized interpolation function whose derivatives appear in a modified total-differential. The parameterized interpolation derivatives are then guaranteed to be continuous along the integration pathline. The parameterized total-differential may then be integrated without requiring a partitioned pathline.

To create a single coordinate-space between two particles, each of the physical, logical, and cell-vertex coordinates must be parameterized; particle states are a collection of these vectors. A simple, linear technique using the variable 's', where $0 \leq s \leq 1$, was selected in this research. The parameterized coordinates, $\bar{X}(s)$, $\bar{\xi}(s)$ and $\bar{X}^{cv}(s)$, then vary linearly along any integration pathline. Integration limits for the parameterized total-differential are the bounding limits of 's'. Integration of the parameterized interpolation total-differential is represented in Equation 6.

$$\int_0^1 \frac{\partial\bar{X}(s)}{\partial s} ds = \int_0^1 \frac{\partial\bar{X}}{\partial\bar{\xi}}(\bar{\xi}(s), \bar{X}^{cv}(s)) \frac{\partial\bar{\xi}(s)}{\partial s} ds + \int_0^1 \frac{\partial\bar{X}}{\partial\bar{X}^{cv}}(\bar{\xi}(s)) \frac{\partial\bar{X}^{cv}(s)}{\partial s} ds \quad (6)$$

Solution of Equation 6 requires an integration pathline defined between two particles end-states. An integration pathline for the parameterized total-differential traverses through the $(\bar{\xi}, \bar{X}^{cv})$ plane since these vectors are the arguments of the interpolation function as defined for spatial transformation: $\bar{X} = \bar{X}(\bar{\xi}, \bar{X}^{cv})$. While the parameterization function does not prescribe the shape of the integration pathline, it does define the parameterization variable's behavior along any path between two particle positions. Three unique integration pathlines were selected by this research to solve Equation 6: direct, upper-step, and lower-step integration pathlines.

Discrete-Expansions

The purpose of this section is to review the discrete-expansions for linear and bilinear interpolation developed using the total-differential method. Details of the development process, including integration the parameterized total-differential, are provided in References [67,68]. The bilinear discrete-expansions will be presented first; the linear interpolation solutions are often subsets of the non-linear solutions. At the end of this section, the general form of these discrete-expansions will be discussed. The final section of this report will discuss the application of discrete-expansions for numerical analysis and localization within particle methods.

Bilinear Interpolation

Direct Pathline The first integration pathline used to solve Equation 6 is a direct line between States 1 and 2; see Figure 4. The two discrete-expansions for bilinear interpolation most easily obtained using the direct integration pathline are presented in Equation 7.

$$\begin{aligned}
 \Delta \bar{X} &= \frac{\partial \bar{X}}{\partial \bar{\xi}}(\hat{\xi}, \hat{X}^{cv}) \Delta \bar{\xi} + \frac{\partial \bar{X}}{\partial \bar{X}^{cv}}(\hat{\xi}) \Delta \bar{X}^{cv} + \frac{1}{4} \frac{\partial^2 \bar{X}}{\partial \bar{\xi} \partial \eta}(\Delta \bar{X}^{cv}) \Delta \bar{\xi} \Delta \eta \\
 \Delta \bar{X} &= \frac{1}{2} \frac{\partial \bar{X}}{\partial \bar{\xi}}(\bar{\xi}_1, \bar{X}_1^{cv}) \Delta \bar{\xi} + \frac{1}{2} \frac{\partial \bar{X}}{\partial \bar{X}^{cv}}(\bar{\xi}_1) \Delta \bar{X}^{cv} \\
 &+ \frac{1}{2} \frac{\partial \bar{X}}{\partial \bar{\xi}}(\bar{\xi}_2, \bar{X}_2^{cv}) \Delta \bar{\xi} + \frac{1}{2} \frac{\partial \bar{X}}{\partial \bar{X}^{cv}}(\bar{\xi}_2) \Delta \bar{X}^{cv} - \frac{1}{2} \frac{\partial^2 \bar{X}}{\partial \bar{\xi} \partial \eta}(\Delta \bar{X}^{cv}) \Delta \bar{\xi} \Delta \eta
 \end{aligned} \tag{7}$$

Upper-Step Pathline The second integration pathline used to solve Equation 6 is comprised of two line-segments between States 1 and 2. The first pathline segment is a line of constant $\bar{\xi}$ from State 1 to State A; see Figure 4. The second pathline segment is a line of constant \bar{X}^{cv} from State A to State 2. These two pathline segments form an upper-step within the $(\bar{\xi}, \bar{X}^{cv})$ plane. The three discrete-expansions for bilinear interpolation most easily obtained using the upper-step integration pathline are presented in Equation 8.

$$\begin{aligned}
 \Delta \bar{X} &= \frac{\partial \bar{X}}{\partial \bar{\xi}}(\hat{\xi}, \bar{X}_2^{cv}) \Delta \bar{\xi} + \frac{\partial \bar{X}}{\partial \bar{X}^{cv}}(\bar{\xi}_1) \Delta \bar{X}^{cv} \\
 \Delta \bar{X} &= \frac{\partial \bar{X}}{\partial \bar{\xi}}(\bar{\xi}_1, \bar{X}_2^{cv}) \Delta \bar{\xi} + \frac{\partial^2 \bar{X}}{\partial \bar{\xi} \partial \eta}(\bar{X}_2^{cv}) \Delta \bar{\xi} \Delta \eta + \frac{\partial \bar{X}}{\partial \bar{X}^{cv}}(\bar{\xi}_1) \Delta \bar{X}^{cv} \\
 \Delta \bar{X} &= \frac{\partial \bar{X}}{\partial \bar{\xi}}(\bar{\xi}_2, \bar{X}_2^{cv}) \Delta \bar{\xi} - \frac{\partial^2 \bar{X}}{\partial \bar{\xi} \partial \eta}(\bar{X}_2^{cv}) \Delta \bar{\xi} \Delta \eta + \frac{\partial \bar{X}}{\partial \bar{X}^{cv}}(\bar{\xi}_1) \Delta \bar{X}^{cv}
 \end{aligned} \tag{8}$$

Lower-Step Pathline The third integration pathline used to solve Equation 6 is comprised of two line-segments between States 1 and 2. The first pathline segment is a line of constant \bar{X}^{cv} from State 1 to State B; see Figure 4. The second pathline segment is a line of constant $\bar{\xi}$ from State B to State 2. These two pathline segments form a lower-step within the $(\bar{\xi}, \bar{X}^{cv})$ plane. The three discrete-expansions for bilinear interpolation most easily obtained using the lower-step integration pathline are presented in Equation 9.

$$\begin{aligned}\Delta\bar{X} &= \frac{\partial\bar{X}}{\partial\bar{\xi}}(\hat{\bar{\xi}}, \bar{X}_1^{cv}) \Delta\bar{\xi} + \frac{\partial\bar{X}}{\partial\bar{X}^{cv}}(\bar{\xi}_2) \Delta\bar{X}^{cv} \\ \Delta\bar{X} &= \frac{\partial\bar{X}}{\partial\bar{\xi}}(\bar{\xi}_1, \bar{X}_1^{cv}) \Delta\bar{\xi} + \frac{\partial^2\bar{X}}{\partial\bar{\xi}\partial\eta}(\bar{X}_1^{cv}) \Delta\bar{\xi} \Delta\eta + \frac{\partial\bar{X}}{\partial\bar{X}^{cv}}(\bar{\xi}_2) \Delta\bar{X}^{cv} \\ \Delta\bar{X} &= \frac{\partial\bar{X}}{\partial\bar{\xi}}(\bar{\xi}_2, \bar{X}_1^{cv}) \Delta\bar{\xi} - \frac{\partial^2\bar{X}}{\partial\bar{\xi}\partial\eta}(\bar{X}_1^{cv}) \Delta\bar{\xi} \Delta\eta + \frac{\partial\bar{X}}{\partial\bar{X}^{cv}}(\bar{\xi}_2) \Delta\bar{X}^{cv}\end{aligned}\quad (9)$$

Linear Interpolation

Direct Pathline The three discrete-expansions for linear interpolation most easily obtained using the direct integration pathline are presented in Equation 10.

$$\begin{aligned}\Delta\bar{X} &= \frac{\partial\bar{X}}{\partial\bar{\xi}}(\hat{X}^{cv}) \Delta\bar{\xi} + \frac{\partial\bar{X}}{\partial\bar{X}^{cv}}(\hat{\bar{\xi}}) \Delta\bar{X}^{cv} \\ \Delta\bar{X} &= \frac{\partial\bar{X}}{\partial\bar{\xi}}(\bar{X}_1^{cv}) \Delta\bar{\xi} + \frac{\partial\bar{X}}{\partial\bar{\xi}}(\Delta\bar{X}^{cv}) \Delta\bar{\xi} + \frac{\partial\bar{X}}{\partial\bar{X}^{cv}}(\bar{\xi}_1) \Delta\bar{X}^{cv} \\ \Delta\bar{X} &= \frac{\partial\bar{X}}{\partial\bar{\xi}}(\bar{X}_2^{cv}) \Delta\bar{\xi} - \frac{\partial\bar{X}}{\partial\bar{\xi}}(\Delta\bar{X}^{cv}) \Delta\bar{\xi} + \frac{\partial\bar{X}}{\partial\bar{X}^{cv}}(\bar{\xi}_2) \Delta\bar{X}^{cv}\end{aligned}\quad (10)$$

Upper-Step Pathline The single discrete-expansion for linear interpolation most easily obtained using the upper-step integration pathline is presented in Equation 11.

$$\Delta\bar{X} = \frac{\partial\bar{X}}{\partial\bar{\xi}}(\bar{X}_2^{cv}) \Delta\bar{\xi} + \frac{\partial\bar{X}}{\partial\bar{X}^{cv}}(\bar{\xi}_1) \Delta\bar{X}^{cv}\quad (11)$$

Lower-Step Pathline The single discrete-expansion for linear interpolation most easily obtained using the lower-step integration pathline is presented in Equation 12.

$$\Delta\bar{X} = \frac{\partial\bar{X}}{\partial\bar{\xi}}(\bar{X}_1^{cv}) \Delta\bar{\xi} + \frac{\partial\bar{X}}{\partial\bar{X}^{cv}}(\bar{\xi}_2) \Delta\bar{X}^{cv}\quad (12)$$

The discrete-expansions in Equations 7-12, eight for bilinear interpolation and five for the linear function, are similar to a Taylor's series; they are combinations of scaled derivatives. For these two multi-linear functions of finite order, the expansions have a limited number of terms; for bilinear interpolation, only first and mixed second-order derivatives are non-zero. Arguments of the interpolation derivatives include particle end-state logical and cell-vertex coordinates, or their averages: $\hat{\xi} = (\bar{\xi}_1 + \bar{\xi}_2)/2$ and $\hat{X}^{cv} = (\bar{X}_1^{cv} + \bar{X}_2^{cv})/2$. Other arguments include the finite-difference in the cell-vertex coordinates: $\Delta\bar{X}^{cv}$. While the transformation matrices are scaled by the finite-difference vectors $\Delta\bar{\xi}$ and $\Delta\bar{X}^{cv}$, the second-order derivative, the vector $\partial^2\bar{X}/\partial\xi\partial\eta$, is multiplied by the two scalar finite-differences $\Delta\xi$ and $\Delta\eta$.

The discrete-expansions obtained using the upper-step pathline, Equations 8 and 11, are similar to those obtained using the lower-step pathline, Equations 9 and 12. Evaluation of the interpolation derivatives in these expansions is easily visualized using Figure 4. Within Equations 8 and 11, the derivatives with respect to $\bar{\xi}$, both $\partial\bar{X}/\partial\bar{\xi}$ and $\partial^2\bar{X}/\partial\xi\partial\eta$, are evaluated at \bar{X}_2^{cv} ; the logical-coordinates vary along the pathline segment where \bar{X}^{cv} is fixed at State 2. Similarly, within Equations 8 and 11 the geometry-transformation matrix, $\partial\bar{X}/\partial\bar{X}^{cv}$, is evaluated at $\bar{\xi}_1$; the cell-vertex coordinates vary along the pathline segment where $\bar{\xi}$ is fixed at State 1. The lower-step discrete-expansions, Equations 9 and 12, are nearly identical to the upper-step expansions. While the form of these expansions are identical, the interpolation derivatives are evaluated at opposite particle end-states; these integration pathlines are exact mirror images of each other.

Since linear interpolation is more simple than a bilinear function, the discrete-expansions in Equations 10-12 represent a simplification of the multi-linear expansions in Equations 7-9. The first discrete-expansion in Equation 10 is the linear version of the direct-pathline bilinear expansions in Equation 7. The discrete-expansion in Equation 11 is the linear version of the upper-step bilinear expansions in Equation 8. Similarly, the discrete-expansion in Equation 12 is the linear version of the lower-step bilinear expansions in Equation 9.

However, unique discrete-expansion formulations are possible for linear interpolation; the transformation matrices are easily manipulated since they are linear functions of $\bar{\xi}$ and \bar{X}^{cv} . The second and third linear discrete-expansions in Equation 10 include transformation matrices that are evaluated at the identical particle end-state. A second Jacobian matrix, evaluated with $\Delta\bar{X}^{cv}$, also appears in these expansions. The form of these two expansions is not repeated in the bilinear solutions. These two linear expansions, obtained using the direct integration pathline, are also related to the expansions developed using the upper and lower-step pathlines. The second expansion in Equation 10 is equivalent to the upper-step expansion in Equation 11. Similarly, the third expansion in Equation 10 is equivalent to the lower-step expansion in Equation 12.

The total-differential and finite-difference methods of developing discrete-expansions produce identical results for similar computational cells and interpolation functions. The second expansion in Equation 8 is the two-dimensional version of the trilinear expansion obtained using the finite-difference method [64-66]. Bilinear interpolation defined in quadrilateral cells is a subset of the trilinear function defined in three-dimensional hexahedral cells. Furthermore, the hierarchy of multi-linear interpolation functions dictates that the expansion in Equation 11 is the linear version of the bilinear expansions in Equation 8 and, thus, the single trilinear expansion. Each of the two-dimensional discrete-expansions were obtained using the upper-step pathline.

Discussion

Particle methods require expansions of interpolation functions for numerical analysis and logical-coordinate evaluation. Application of the discrete-expansions developed herein for these purposes is beyond the scope of this report. Verification of the new expansions, however, is provided in Reference [67] for linear interpolation and in Reference [68] for bilinear interpolation. Within the following sections, application of linear and bilinear discrete-expansions for numerical analysis and localization within particle methods is outlined and discussed.

Numerical Analysis

The goal of numerical analysis, an analytical investigation of a computational model, includes establishing the model's mathematical consistency and numerical accuracy. While estimates of these measures are possible, analytical proof of a computational model's consistency and accuracy is preferred. A particle method's consistency and accuracy are based upon its leading-order error term, which is evaluated by substituting series expansions for all discrete-terms within the model. A Taylor's series, however, is not a valid expansion for coupled multi-linear interpolation functions. Instead, a discrete-expansion is required to complete numerical analyses of computational models that use interpolation.

For example, numerical analyses of reactive particle methods require a discrete-expansion of a velocity-interpolation function; these methods compute particle trajectories by interpolating from a discrete velocity field. Furthermore, all numerical analyses require that the discrete-expansion must be written relative to a single state, defined here as State 1. Using multi-step integration methods, however, a reactive particle's velocity might be evaluated in a separate, non-contiguous grid cell, defined here as State 2. The objective is then to write discrete-expansion of the velocity-interpolation function from State 1 to State 2: $\bar{V}_2 = \bar{V}_1 + f(\bar{\xi}_1, \bar{V}_1^{CV})$.

Any one of the above discrete-expansions may be used for numerical analysis; each expansion is valid throughout a discretized domain. One obvious choice would be the common

expansion obtained using both the finite-difference and total-differential development methods. For linear interpolation, the common discrete-expansion, originally presented in Equation 11, is repeated in Equation 13 for an interpolated velocity function.

$$\bar{V}(\bar{\xi}_2, \bar{V}_2^{cv}) = \bar{V}(\bar{\xi}_1, \bar{V}_1^{cv}) + \frac{\partial \bar{V}}{\partial \bar{\xi}}(\bar{V}_2^{cv}) \Delta \bar{\xi} + \frac{\partial \bar{V}}{\partial \bar{V}^{cv}}(\bar{\xi}_1) \Delta \bar{V}^{cv} \quad (13)$$

For bilinear interpolation, the common discrete-expansion, originally presented as the second expression in Equation 8, is repeated in Equation 14 for an interpolated velocity function.

$$\begin{aligned} \bar{V}(\bar{\xi}_2, \bar{V}_2^{cv}) &= \bar{V}(\bar{\xi}_1, \bar{V}_1^{cv}) \\ &+ \frac{\partial \bar{V}}{\partial \bar{\xi}}(\bar{\xi}_1, \bar{V}_2^{cv}) \Delta \bar{\xi} + \frac{\partial^2 \bar{V}}{\partial \bar{\xi} \partial \eta}(\bar{V}_2^{cv}) \Delta \bar{\xi} \Delta \eta + \frac{\partial \bar{V}}{\partial \bar{V}^{cv}}(\bar{\xi}_1) \Delta \bar{V}^{cv} \end{aligned} \quad (14)$$

For numerical analysis, discrete-expansions must be defined at a single state but each expansion above includes interpolation derivatives defined with State 2 variables; $\partial \bar{V}(\bar{V}_2^{cv})/\partial \bar{\xi}$ in Equation 13, and both $\partial \bar{V}(\bar{\xi}_1, \bar{V}_2^{cv})/\partial \bar{\xi}$ and $\partial^2 \bar{V}(\bar{V}_2^{cv})/\partial \bar{\xi} \partial \eta$ in Equation 14. The appropriate recursive application of the linear and bilinear expansions in Equations 13 and 14 can transform the mixed-state interpolated velocity into a State 1 function: $\bar{V}(\bar{\xi}_1, \bar{V}_2^{cv}) = f(\bar{V}^{cv}(\bar{\xi}_1, \bar{V}_1^{cv}))$. This single-state interpolated velocity function can be substituted back into Equations 13 and 14, and the computational model's numerical analysis may then be completed.

For computational models that use interpolation, discrete-expansions represent a key advancement in the ability to both analyze existing models and develop advanced models. For existing computational models, discrete-expansions provide the capacity to analytically evaluate their mathematical consistency and numerical accuracy. By providing an analytical description of a model's leading-order error term, discrete-expansions also provide the capacity to develop advanced computational models. The leading-order error term of an existing model may be used to create a new, advanced computational model that provides greater numerical accuracy.

Logical-Coordinate Evaluation

Logical-coordinate evaluation is the transformation of a physical-space position vector into a cell-based, logical-coordinate system. Interpolation functions are often used for spatial transformation because they can provide a relationship between physical and logical coordinates. Discrete-expansions represent the mathematical expression that allows interpolation functions to evaluate a particle's logical-coordinates. For linear interpolation, the discrete-expansion originally presented in Equation 11 may be rewritten for this purpose as presented in Equation 15.

$$\frac{\partial \bar{X}}{\partial \bar{\xi}}(\bar{X}_2^{cv}) \Delta \bar{\xi} = (\bar{X}_2 - \bar{X}_1) - \frac{\partial \bar{X}}{\partial \bar{X}^{cv}}(\bar{\xi}_1) \Delta \bar{X}^{cv} \quad (15)$$

For bilinear interpolation, the discrete-expansion originally presented in Equation 8 may be rewritten for logical-coordinate evaluation as presented in Equation 16.

$$\frac{\partial \bar{X}}{\partial \bar{\xi}}(\bar{\xi}_1, \bar{X}_2^{cv}) \Delta \bar{\xi} = (\bar{X}_2 - \bar{X}_1) - \frac{\partial \bar{X}}{\partial \bar{X}^{cv}}(\bar{\xi}_1) \Delta \bar{X}^{cv} - \frac{\partial^2 \bar{X}}{\partial \bar{\xi} \partial \eta}(\bar{X}_2^{cv}) \Delta \xi \Delta \eta \quad (16)$$

Both of these discrete-expansions are valid between two particles, States 1 and 2, located in separate, non-contiguous grid cells. For logical-coordinate evaluation, the coordinate vectors defined at State 1 are known: \bar{X}_1 , $\bar{\xi}_1$ and \bar{X}_1^{cv} . In contrast, the only coordinates known at State 2 are the physical-coordinates of the particle, \bar{X}_2 . The cell-searching portion of the localization algorithm does, however, identify a guessed cell for the particle at State 2, which provides cell-vertex coordinates, \bar{X}_2^{cv} . The only unknown vector in Equations 15 and 16 is the logical-coordinate vector at State 2, $\bar{\xi}_2$, which is the desired solution embedded within $\Delta \bar{\xi} = \bar{\xi}_2 - \bar{\xi}_1$. In general, the vectors $\Delta \bar{\xi}$ and $\Delta \bar{X}^{cv}$ are non-zero finite differences.

The most important feature of Equations 15 and 16 is that the discrete-expansions are defined between two *fixed* particle positions. State 2 is *absolutely* fixed, invariant throughout the localization problem, by the particle's physical-coordinates, \bar{X}_2 . Logical-coordinate evaluation completes the definition of State 2 by providing the vectors $\bar{\xi}_2$ and \bar{X}_2^{cv} . In contrast, State 1 is *arbitrarily* fixed; its position within the computational domain is constrained only by the requirement that $\bar{X}_1 = \bar{X}(\bar{\xi}_1, \bar{X}_1^{cv})$. Therefore, a bound $\bar{\xi}_1$ vector may be selected for use within Equation 16 that guarantees a non-singular Jacobian matrix and, thus, an algorithmically robust evaluation method. Similarly, logical-coordinate evaluation using the linear discrete-expansion is robust; the Jacobian matrix in Equation 15 is not a function of logical-coordinates.

Solution of Equations 15 and 16 for logical-coordinate evaluation is also computationally efficient; all of their interpolation derivatives are constant and only require a single evaluation. Inversion of the Jacobian matrices is only required once. While, the interpolation derivatives within Equations 15 and 16 are not functions of the solution vector, elements of $\bar{\xi}_2$ appear on the right-hand-side of the bilinear discrete-expansion. An iterative solution strategy, one that lags the second-order derivative term, can be applied to Equation 16 to obtain $\Delta \bar{\xi}$. The constant Jacobian matrix can be reused throughout the iterative solution of Equation 16. In contrast, only a single solution of Equation 15 is required for logical-coordinate evaluation using linear interpolation.

Summary

The objective of this research was to develop discrete-expansions for common multi-linear interpolation functions. Five discrete-expansions were developed for linear interpolation defined in triangular cells, and eight discrete-expansions were developed for bilinear interpolation defined in quadrilateral cells. These expansions were developed by parametrically integrating the interpolation function's total-differential between two particles located within separate, non-contiguous grid cells. Discrete-expansions are similar to multi-variable expansions, but unlike Taylor's series, they are valid throughout a discretized domain. For particle methods, discrete-expansions are valid for numerical analyses since they account for interpolation discontinuities across cell boundaries. The use of discrete-expansions for logical-coordinate evaluation also provides an algorithmically robust and computationally efficient particle localization method.

Acknowledgement

This work was sponsored by the Accelerated Strategic Computing Initiative Program at the Los Alamos National Laboratory. Thanks to Forrest B. Brown, John H. Hall and Stephen R. Lee of the Blanca Project for their support of this investigation. Much thanks to James R. Kamm and Gary L. Sandine of the Applied Physics Division for assistance in this research.

References

- 1) Watkins, A. P., "Three-Dimensional Modeling of Gas Flow and Sprays in Diesel Engines," *Computer Simulation for Fluid Flow, Heat and Mass Transfer and Combustion in Reciprocating Engines*, Markatos, N. C., Editor, Hemisphere, Washington, D. C., pp. 193-237, 1989.
- 2) Dukowicz, J. K., "A Particle-Fluid Numerical Model for Liquid Sprays," *Journal of Computational Physics*, Vol. 35, pp. 229-253, 1980.
- 3) Crowe, C. T., Sharma, M. P. and Stock, D. E., "The Particle-Source-In Cell Model for Gas-Droplet Flows," *Journal of Fluids Engineering*, Vol. 99, pp. 325-331, 1977.
- 4) Amsden, A. A. and Hirt, C. W., "Yaqui: An Arbitrary Lagrangian-Eulerian Computer Program for Fluid Flow at All Speeds," Los Alamos National Laboratory Report, LA-5100, 1973.
- 5) Delnoij, E., Lammers, F. A., Kuipers, J. A. M. and van Swaaij, W. P. M., "Dynamic Simulation of Dispersed Gas-Liquid Two-Phase Flow Using a Discrete Bubble Model," *Chemical Engineering Science*, Vol. 52, pp. 1429-1458, 1997.
- 6) Sokolichin, A., Eigenberger, G., Lapin, A. and Lubbert, A., "Dynamic Numerical Simulation of Gas-Liquid Two-Phase Flows: Euler/Euler versus Euler/Lagrange," *Chemical Engineering Science*, Vol. 52, pp. 611-626, 1997.
- 7) Lapin, A. and Lubbert, A., "Numerical Simulation of the Dynamics of Two-Phase Gas-Liquid Flows in Bubble Columns," *Chemical Engineering Science*, Vol. 49, pp. 3661-3674, 1994.
- 8) Trapp, J. A. and Mortensen, G. A., "A Discrete Particle Model for Bubble-Slug Two-Phase Flows," *Journal of Computational Physics*, Vol. 107, pp. 367-377, 1993.
- 9) Webb, C., Que, F. and Senior, P. R., "Dynamic Simulation of Gas-Liquid Dispersion Behavior in a 2-D Bubble Column Using a Graphics Mini-Supercomputer," *Chemical Engineering Science*, Vol. 47, pp. 3305-3312, 1992.
- 10) Rider, W. J. and Kothe, D. B., "A Marker Particle Method for Interface Tracking," Los Alamos Laboratory Report LA-UR-95-1740, 1995.
- 11) Rider, W. J., Kothe, D. B., Mosso, S. J., Cerutti, J. H. and Hochstein, J. I., "Accurate Solution Algorithms for Incompressible Multiphase Flows," AIAA Paper 95-0699, 1995. (Los Alamos Laboratory Report LA-UR-94-3611, 1994.)

References Continued

- 12) Gifford, F. A., Barr, S., Malone, R. C. and Mroz, E. J., "Tropospheric Relative Diffusion to Hemispheric Scales," *Atmospheric Environment*, Vol. 22, pp. 1871-1879, 1988.
- 13) McNider, R. T., Moran, M. D. and Pielke, R. A., "Influence of Diurnal and Inertial Boundary-Layer Oscillations on Long-Range Dispersion," *Atmospheric Environment*, Vol. 22, pp. 2445-2462, 1988.
- 14) Walton, J. J. and MacCracken, M. C., "Preliminary Report on the Global Transport Model GRANTOUR," Lawrence Livermore National Laboratory Report, UCID-19985, 1984.
- 15) Hanna, S. R., "Some Statistics of Lagrangian and Eulerian Wind Fluctuations," *Journal of Applied Meteorology*, Vol. 18, pp. 518-525, 1979.
- 16) Hotchkiss, R. S. and Harlow, F. H., "Air Pollution Transport in Street Canyons," Environmental Protection Agency Report, EPA-R4-73-029, 1973.
- 17) Hirt, C. W. and Cook, J. L., "Calculating Three-Dimensional Flows Around Structures and Over Rough Terrain," *Journal of Computational Physics*, Vol. 10, pp. 324-340, 1972. (Los Alamos National Laboratory Report LA-DC-13289, 1971.)
- 18) Hotchkiss, R. S. and Hirt, C. W., "Particulate Transport in Highly Distorted Three-Dimensional Flow Fields," Los Alamos National Laboratory Report LA-DC-72-364, 1972.
- 19) Hotchkiss, R. S., "The Numerical Calculation of Three-Dimensional Flows of Air and Particulates About Structures," Los Alamos National Laboratory Report LA-DC-13071, 1971.
- 20) Lu, N., "A Semianalytical Method of Path Line Computation for Transient Finite-Difference Groundwater Flow Models," *Water Resources Research*, Vol. 30, pp. 2449-2459, 1994.
- 21) Schafer-Perini, A. L. and Wilson, J. L., "Efficient and Accurate Front Tracking for Two-Dimensional Groundwater Flow Models," *Water Resources Research*, Vol. 27, pp. 1471-1485, 1991.
- 22) Tompson, A. F. B. and Gelhar, L. W., "Numerical Simulation of Solute Transport in Three-Dimensional, Randomly Heterogeneous Porous Media," *Water Resources Research*, Vol. 26, pp. 2541-2562, 1990.

References Continued

- 23) Goode, D. J., "Particle Velocity Interpolation in Block-Centered Finite Difference Groundwater Flow Models," *Water Resources Research*, Vol. 26, pp. 925-940, 1990.
- 24) Pollock, D. W., "Semianalytical Computation of Path Lines for Finite-Difference Models," *Ground Water*, Vol. 26, pp. 743-750, 1988.
- 25) Uffink, G. J. M., "Modeling of Solute Transport with the Random Walk Method," *Groundwater Flow and Quality Modeling*, Custodio, E., Gurgui, A. and Lobo Ferreria, J. P., Editors, D. Reidel Publishing Company, pp. 247-265, 1988.
- 26) Kinzelbach, W., "The Random Walk Method in Pollutant Transport Simulation," *Groundwater Flow and Quality Modeling*, Custodio, E., Gurgui, A. and Lobo Ferreria, J. P., Editors, D. Reidel Publishing Company, pp. 227-245, 1988.
- 27) Shafer, J. M., "Reverse Pathline Calculation of Time-Related Capture Zones in Nonuniform Flow," *Ground Water*, Vol. 25, pp. 283-289, 1987.
- 28) Prickett, T. A., Naymik, T. G. and Lonquist, C. G., "A Random-Walk Solute Transport Model for Selected Groundwater Quality Evaluations," *Bulletin of the Illinois State Water Survey*, Vol. 65, pp. 1-104, 1981.
- 29) Nelson, R. W., "Evaluating the Environmental Consequences of Groundwater Contamination," *Water Resources Research*, Vol. 14, pp. 409-450, 1978.
- 30) Smith, F. G., "A Model of Transient Mixing in a Stirred Tank," *Chemical Engineering Science*, Vol. 52, No. 9, pp. 1459-1478, 1997.
- 31) Howes, T. and Shardlow, P. J., "Simulation of Mixing in Unsteady Flow Through a Periodically Obstructed Channel," *Chemical Engineering Science*, Vol. 52, No. 7, pp. 1215-1225, 1997.
- 32) Sobey, I. J., "Dispersion Caused by Separation During Oscillatory Flow Through a Furrowed Channel," *Chemical Engineering Science*, Vol. 40, No. 11, pp. 2129-2134, 1985.
- 33) Nielson, G. M., Hagen, H. and Muller, H., *Scientific Visualization*, IEEE Computer Society Press, Los Alamitos, CA, 1997.

References Continued

- 34) Wolf, R. S. and Yaeger, L., *Visualization of Natural Phenomena*, Springer-Verlag, New York, 1993.
- 35) Friedhoff, R. M. and Benzon, W., *Visualization: The Second Computer Revolution*, Harry N. Abrams, New York, 1989.
- 36) Nakayama, T. and Mori, M., "An Eulerian Finite Element Method for Time-Dependent Free Surface Problems in Hydrodynamics," *International Journal for Numerical Methods in Fluids*, Vol. 22, pp. 175-194, 1996.
- 37) Viecelli, J. A., "A Computing Method for Incompressible Flows Bounded by Moving Walls," *Journal of Computational Physics*, Vol. 8, pp. 119-143, 1971.
- 38) Amsden, A. A. and Harlow, F. H., "A Simplified MAC Technique for Incompressible Fluid Flow Calculations," *Journal of Computational Physics*, Vol. 6, pp. 322-325, 1970.
- 39) Amsden, A. A. and Harlow, F. H., "The SMAC Method: A Numerical Technique for Calculating Incompressible Fluid Flows," Los Alamos National Laboratory Report LA-4370, 1970.
- 40) Harlow, F. H. and Welch, J. E., "Numerical Calculation of Time-Dependent Viscous Incompressible Flow of Fluid with Free Surface," *Physics of Fluids*, Vol. 8, pp. 2182-2189, 1965.
- 41) Welch, J. E., Harlow, F. H., Shannon, J. P. and Daly, B. J., "The MAC Method: A Computing Technique for Solving Viscous, Incompressible, Transient Fluid-Flow Problems Involving Free Surfaces," Los Alamos National Laboratory Report LA-3425, 1965.
- 42) Tryggvason, G., Bunner, B., Juric, D., Tauber, W., Nas, S., Han, J., Al-Rawahi, N., and Jan, Y., "A Front Tracking Method for the Computations of Multiphase Flow," *Journal of Computational Physics*, Review Paper, Published Spring 2001.
- 43) Udaykumar, H. S., Kan, H. C., Shyy, W. and Tran-Son-Tay, R., "Multiphase Dynamics in Arbitrary Geometries on Fixed Cartesian Grids," *Journal of Computational Physics*, Vol. 137, pp. 366-405, 1997.
- 44) Udaykumar, H. S., Shyy, W. and Rao, M. M., "ELAFINT: A Mixed Eulerian-Lagrangian Method for Fluid Flows with Complex and Moving Boundaries," *International Journal for Numerical Methods in Fluids*, Vol. 22, pp. 691-712, 1996.

References Continued

- 45) Udaykumar, H. S. and Shyy, W., "A Grid-Supported Marker Particle Scheme for Interface Tracking," *Numerical Heat Transfer, Part B*, Vol. 27, pp. 127-153, 1995.
- 46) Unverdi, S. O. and Tryggvason, G., "Computations of Multi-Fluid Flows," *Physica D*, Vol. 60, pp. 70-83, 1992.
- 47) Unverdi, S. O. and Tryggvason, G., "A Front-Tracking Method for Viscous, Incompressible, Multi-Fluid Flows," *Journal of Computational Physics*, Vol. 100, pp. 25-37, 1992.
- 48) Miyata, H., "Finite-Difference Simulation of Breaking Waves," *Journal of Computational Physics*, Vol. 65, pp. 179-214, 1986.
- 49) Darmofal, D. L. and Haimes, R., "An Analysis of 3D Particle Path Integration Algorithms," *Journal of Computational Physics*, Vol. 123, pp. 182-195, 1996.
- 50) Cheng, H. P., Cheng, J. R., and Yeh, G. T., "A Particle Tracking Technique for the Lagrangian-Eulerian Finite Element Method in Multi-Dimensions," *International Journal for Numerical Methods in Engineering*, Vol. 39, pp. 1115-1136, 1996.
- 51) Fairfield, M. S., "Three-Dimensional Visualization of Reactive Flows in Complex Geometries," *High Performance Computing, Grand Challenges in Computer Simulation*, Tentner, A. M., Editor, Simulations Councils, pp. 424-427, 1995. (Los Alamos National Laboratory Report LAUR-95-0251, 1995.)
- 52) Murman, E. M. and Powell, K. G., "Trajectory Integration in Vortical Flows," *AIAA Journal*, Vol 27, pp. 982-984, 1989.
- 53) Pracht, W. E. and Brackbill, J. U., "BAAL: A Code for Calculating Three-Dimensional Fluid Flows at All Speeds with an Eulerian-Lagrangian Computing Mesh," Los Alamos National Laboratory Report LA-6342, 1976.
- 54) Wang, J., Kondrashov, D., Liewer, P. C., and Karmesin, S. R., "Three-Dimensional Deformable Grid Electromagnetic Particle-In-Cell for Parallel Computers," *Journal of Plasma Physics*, Vol. 61. pp. 367-389, 1999.
- 55) Brock, J. S. and Painter, J. W., and Kothe, D. B., "Tracer-Particle Advection: Algorithm Components and Implementation Methods," Los Alamos National Laboratory Report LA-UR-98-5659, 1998.

References Continued

- 56) Brock, J. S. and Painter, J. W., "Tracer-Particle Advection: Components, Choices, and a New Alternative," Los Alamos National Laboratory Report LA-UR-98-4691, 1998.
- 57) Shirayama, S., "Processing of Computed Vector Fields for Visualization," *Journal of Computational Physics*, Vol. 106, pp. 30-41, 1993.
- 58) Allievi, A. and Bermejo, R., "A Generalized Particle-Search Algorithm for Arbitrary Grids," *Journal of Computational Physics*, Vol. 132, pp. 157-166, 1997.
- 59) Lohner, R., "Robust, Vectorized Search Algorithms for Interpolation on Unstructured Grids," *Journal of Computational Physics*, Vol. 118, pp. 380-387, 1995.
- 60) Westerman, T., "Localization Schemes in 2D Boundary-Fitted Grids," *Journal of Computational Physics*, Vol. 101, pp. 307-313, 1992.
- 61) Lohner, R. and Ambrosiano, J. "A Vectorized Particle Tracer for Unstructured Grids," *Journal of Computational Physics*, Vol. 91, pp. 22-31, 1990.
- 62) Wilson, T. L., "LINTERP: A Numerical Algorithm for Interpolating Quadrilateral and Hexahedral Meshes," Los Alamos National Laboratory Report LA-11902-MS, 1990.
- 63) Brackbill, J. U., and Ruppel, H. M., "FLIP: A Method for Adaptively Zoned, Particle-in-Cell Calculations of Fluid Flows in Two Dimensions," *Journal of Computational Physics*, Vol. 65, pp. 314-343, 1986.
- 64) Brock, J. S., "A Finite-Difference Logical-Coordinate Evaluation Method For Particle Localization," *Progress of Theoretical Physics*, Sup. 138, pp. 40-42, 2000. (Los Alamos National Laboratory Report LA-UR-99-6493, 1999.)
- 65) Brock, J. S., "A New Logical-Coordinate Evaluation Method For Particle Localization," Los Alamos National Laboratory Report LA-UR-99-5355, 1999.
- 66) Brock, J. S., "Comparing Logical-Coordinate Evaluation Methods," Los Alamos National Laboratory Report LA-UR-99-5354, 1999.
- 67) Wiseman, J. R. and Brock, J. S., "Integrating a Linear Interpolation Function Across Triangular Cell Boundaries," Los Alamos National Laboratory Report LA-UR-00-3330, 2000
- 68) Brock, J. S., "Integrating a Bilinear Interpolation Function Across Quadrilateral Cell Boundaries," Los Alamos National Laboratory Report LA-UR-00-3329, 2000.

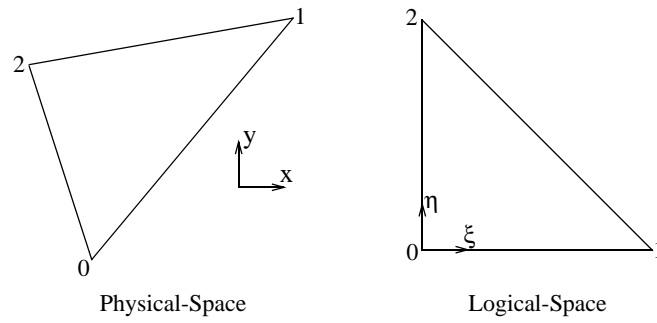
Figures

Figure 1: Coordinate Transformation
for Triangular Cell Geometries

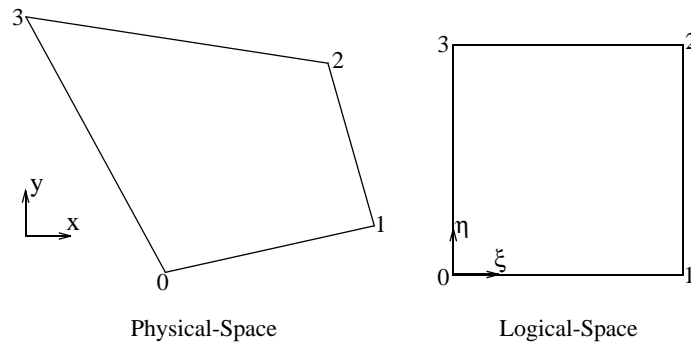


Figure 2: Coordinate Transformation
for Quadrilateral Cell Geometries

Figures Continued

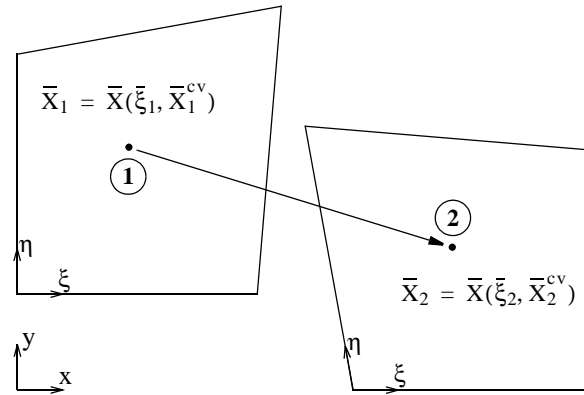


Figure 3: Limits of Integration

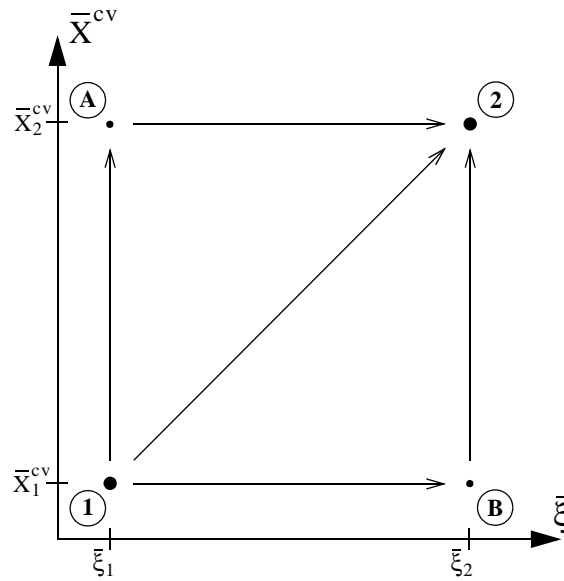


Figure 4: Integration Pathlines